

## Modelling the influence of faults on a developing river system

### 1. Introduction

This numerical study aims to clarify if and how a system of faults may influence the development of a river network. We simulate the effect of varying angles between riverbed and fault on flow direction, and for which configuration a deflection of the river is possible. We also compare the influences of uplift and of high erodibility zones on the deviation of river networks.

This study has a direct application. The highly active Pamir orogen is penetrated by sub-parallel faults. The main rivers of the Pamir flow from east to west, following the fault system. They join the river Panj, that abruptly turns at 71.5° longitude from east-west direction to the north. An old river bed in direction to south-west can be observed at the sudden turn. So far it is unknown, how strong such a fault system influences a river network. Is it possible that the east-west fault system forced the rivers in that direction? Might the Panj river have changed its direction due to a river capturing event, induced by a recently-forming fault?

### 2. The river and fault system in the Pamir

On the geological map, one can see the highly complex fault system of the Pamir orogen. The river system reveals a structure, that seems to follow the fault system

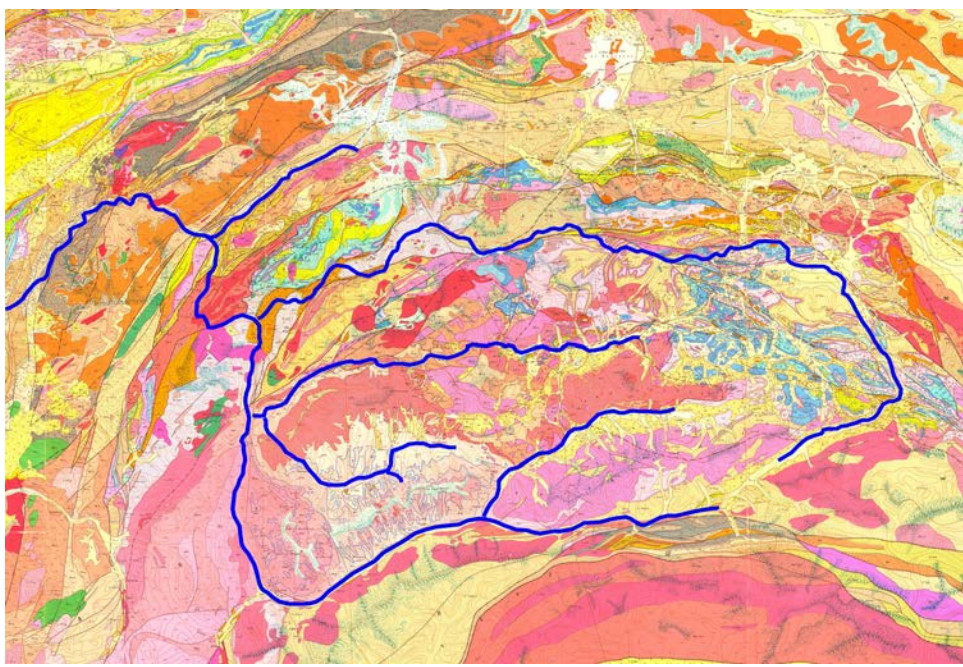


Fig.1: Geological map of the Pamir orogen, Rivers are marked in deep blue

### 6. The influence of the incision rate on a developing river system

The figures show simulated topographies of a developing river network after 50.000y of uplift and surface evolution. The start topography, explained in box no. 5, is uplifted up to 1mm/y. The angle between rivers and faults is 70°.

The models reflect the natural behavior of river networks. In the case at top the uplift exceeds the incision and forces the main channels into a fault. In the model at the bottom, the incision rate is much stronger than the uplift. The channel network gets hardly affected by the fault system. The model in the middle shows a river system partly influenced, partly uninfluenced by the fault system. Such channel systems can be observed in many regions.

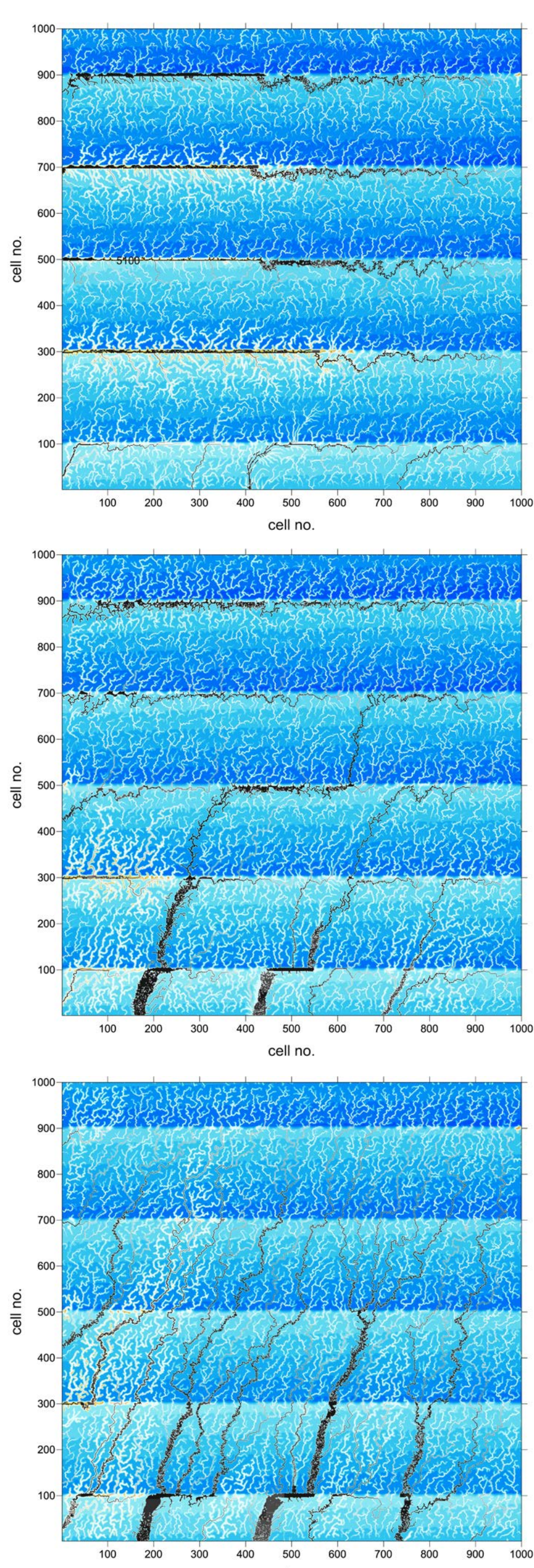


Fig.6: Simulated topographies of a developing river network after 50.000y of uplift and surface evolution. The main rivers are marked in black. The angle between rivers and faults is 70°. The incision rate in the model at bottom is twice as high, as in the model in the middle and 3 times higher than in the model at the top.

### 3. Numerical modelling technique

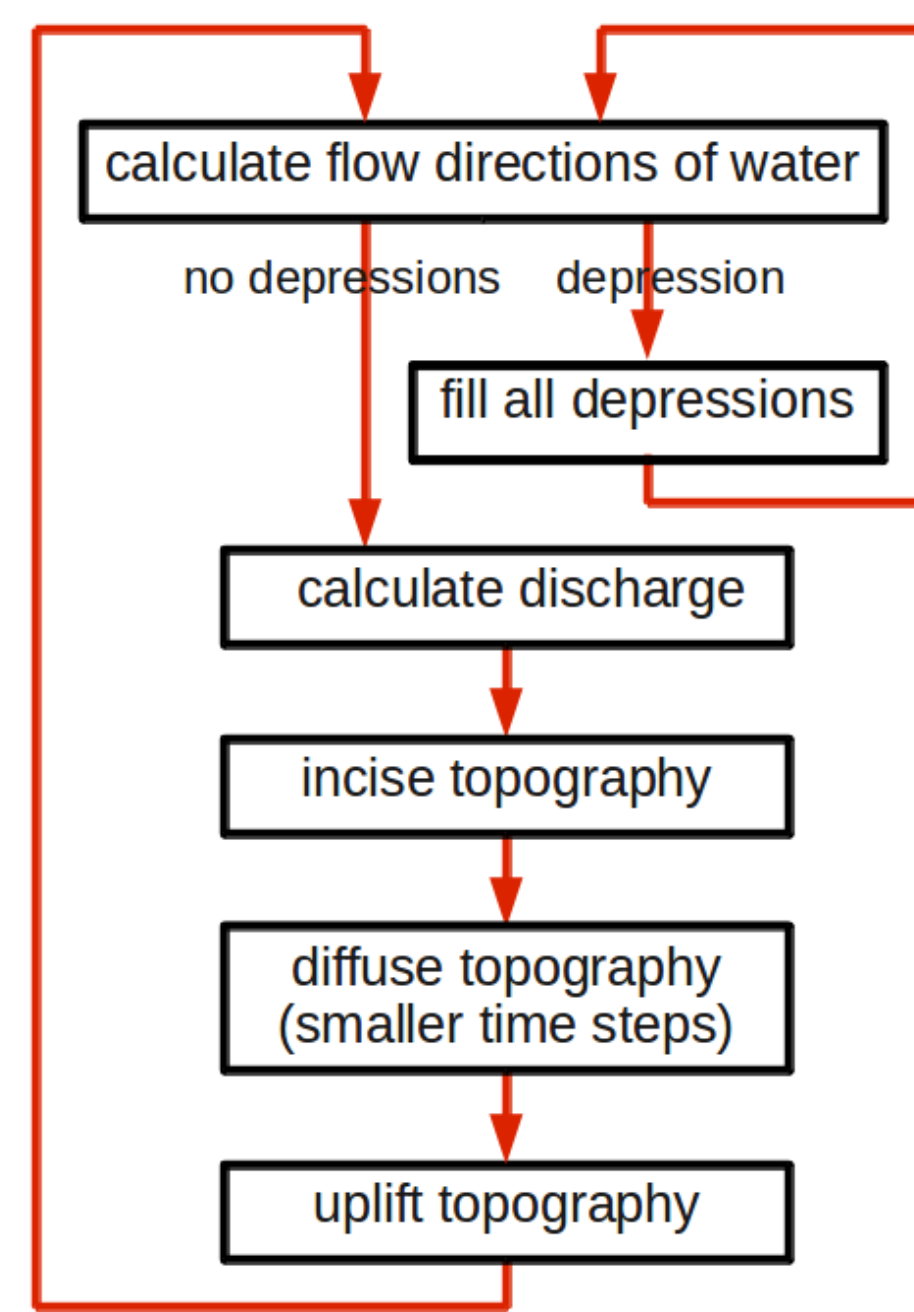


Fig.2: Scheme of erosion algorithm

Here, we present a new, fast Surface Evolution Model (SEM). We follow the concept of the cellular automaton (Beaumont), implemented on a regular Eulerian grid.

In each time step, the surface uplift is added. A modern filling algorithm (Tachikawa et al.) is applied, that adds further offsets to guarantee a flow direction (D8 algorithm by O'Callaghan) in all cells. By counting the number of inflowing streams, the springs are identified. Taking a starting point in each of the springs, it is relatively fast to evaluate the drainage area in each cell. The drainage area, as well as the slope, which is calculated via central differences, are needed for the incision algorithm.

Up to now, the model incorporates long-range processes in the form of bed-rock incision, as well as short-range processes in the form of hillslope-dependent diffusion. We developed a supply-limited incision model that starts to incise from a threshold of drainage area. In all incised cells, the eroded material is washed away immediately. To take the slope dependence of erosion into account, we adopt Beaumont's implementation of the widely known diffusion equation, and attach to the sediment fluxes  $q_s$  a slope dependent factor. This factor rests upon Roering's suggestion of including a critical hillslope gradient  $S_c$ .

Furthermore, the SEM offers a new feature, that allows incision of not only one cell width, but of the whole river valley. This lateral abrasion routine avoids a time consuming multiple flow direction algorithm, but gives a more natural topography and allows working with real Digital Elevation Models. In addition, the numerical model enables headward erosion.

$$\frac{\delta h}{\delta t} = \kappa_{rb} \cdot Q^m S^n$$

Bedrock incision

$$\frac{\delta h}{\delta t} = -\nabla \cdot \underline{q}_s$$

Hillslope diffusion

$$\underline{q}_s = \kappa_{hs} \cdot \nabla h \cdot \left[ 1 - \left( \frac{|\nabla h|}{S_c} \right)^2 \right]^{-1} \text{ for } |\nabla h| < S_c$$

Slope dependent diffusive flux

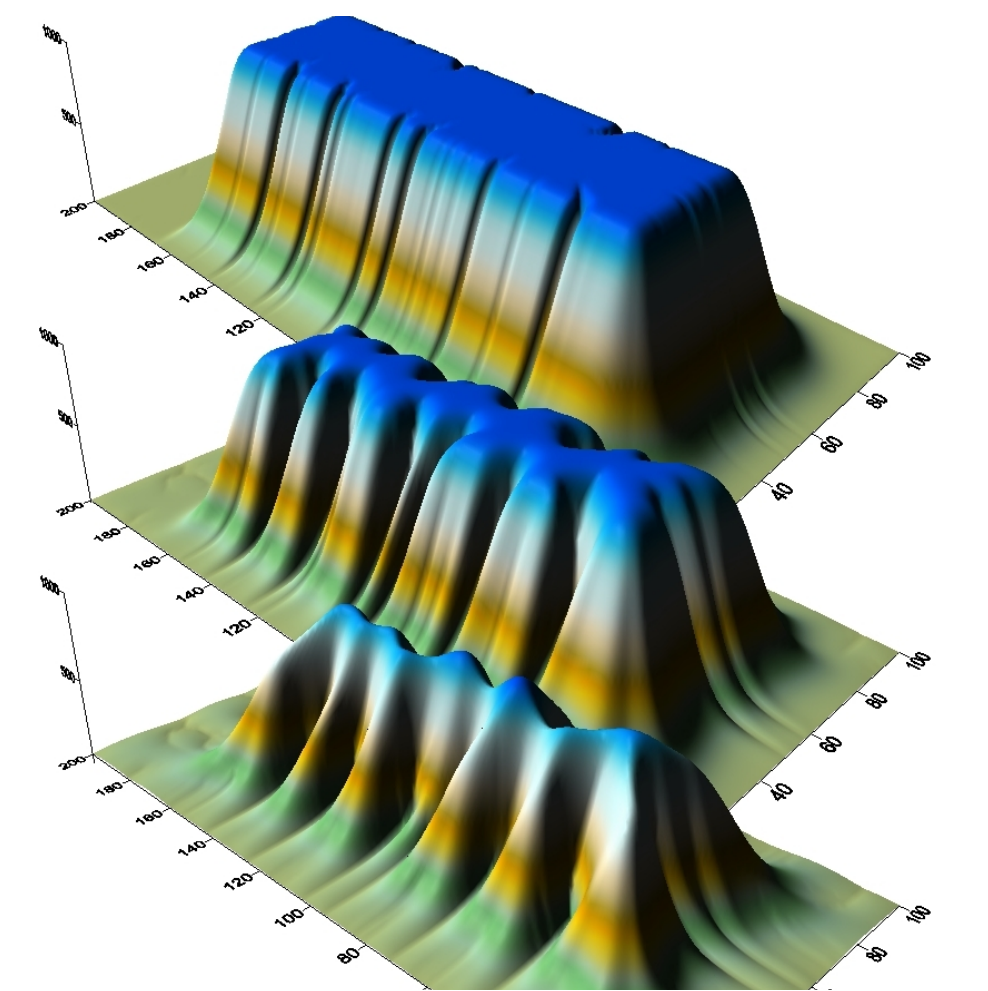


Fig.3: Three points in time: Gaussian shaped uplifting ridge with plateau and white noise. The spatial resolution of the model is 100 x 50 cells of 1000m x 1000m and works with time steps of 250y.

### 4. Algorithm Extension: Lateral abrasion routine

Usually, SEM incise a channel of exactly one cell width.

We extended the algorithm that calculates the water discharge, to guarantee incision in a natural way. The new algorithm spreads the water discharge over several cells, dependent on the amount of water and the height difference to the neighbour cells. Hence, the incision acts in several cells around the calculated trace and therefore enlarges the channel width.

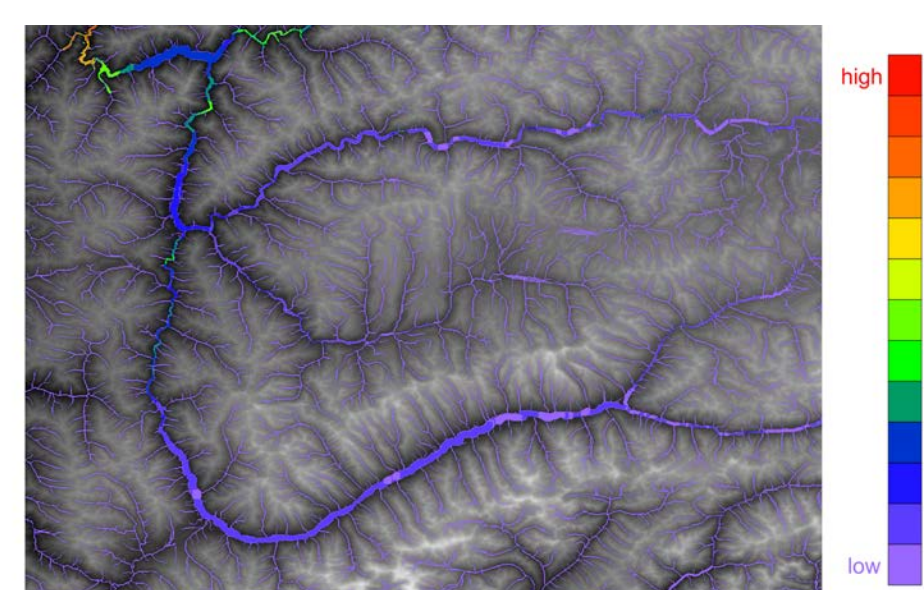


Fig.4: Map of the Pamir orogen with high water discharges, computed by the new SEM. The colour scale labels the amount of water. The unit depends on the precipitation rate.

### 5. The model

We simulate an inclined plane with white noise and faults. The inclination angle defines the main flow direction of the arising rivers. The faults are modelled as regions of hundred times increased erodibility with fault-bounded block rotations. Fig.3 shows the analytically imposed uplift, that is coupled to the introduced Surface Evolution Model (SEM).

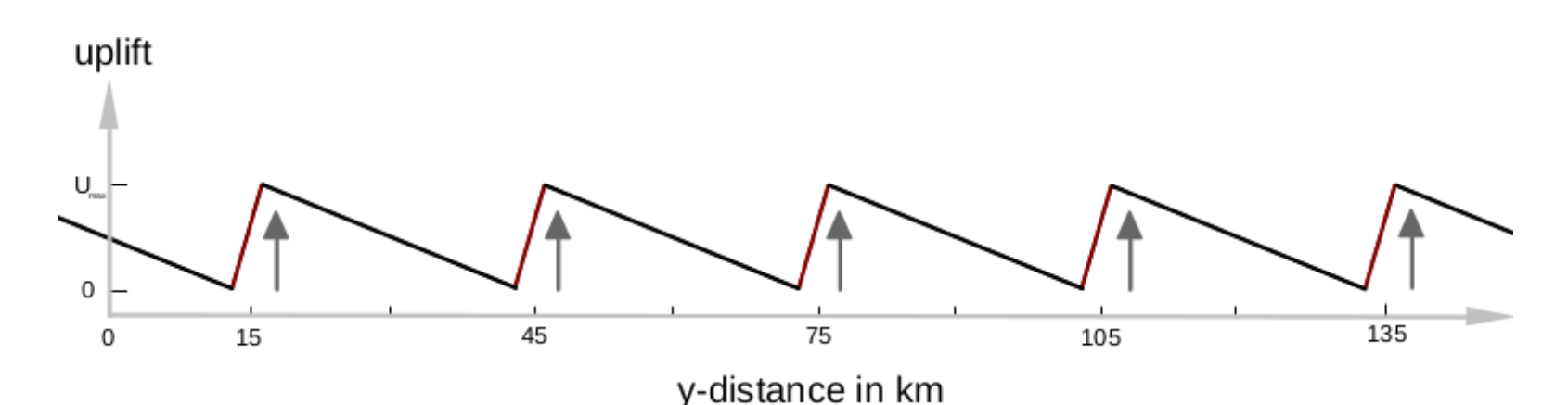


Fig.5: Cross section through the uplift model parallel to the y-axis. Brown regions mark high erodibility zones. Zero uplift is reached in exactly five cells. The uplift is constant in x-direction.

### 7. The influence of the angle between rivers and faults on a developing river system

We adopt the uplift and incision strength of the central model in box no. 6, to study the effect of the angle between faults and channels. With given uplift-incision relation the shown models present the importance of the deflection angle. Here, at 60° all rivers get captured and deflected in fault direction. At 70° the channels get partly captured, partly they stay uninfluenced by the faults. At 80° a river capturing event is hardly possible.

These results lead to the conclusion, that river capturing by faults is highly sensitive to the deflection angle. Hence, just very strong uplift rates can lead to river capturing with a deflection angle of 90°, like in the Pamir.

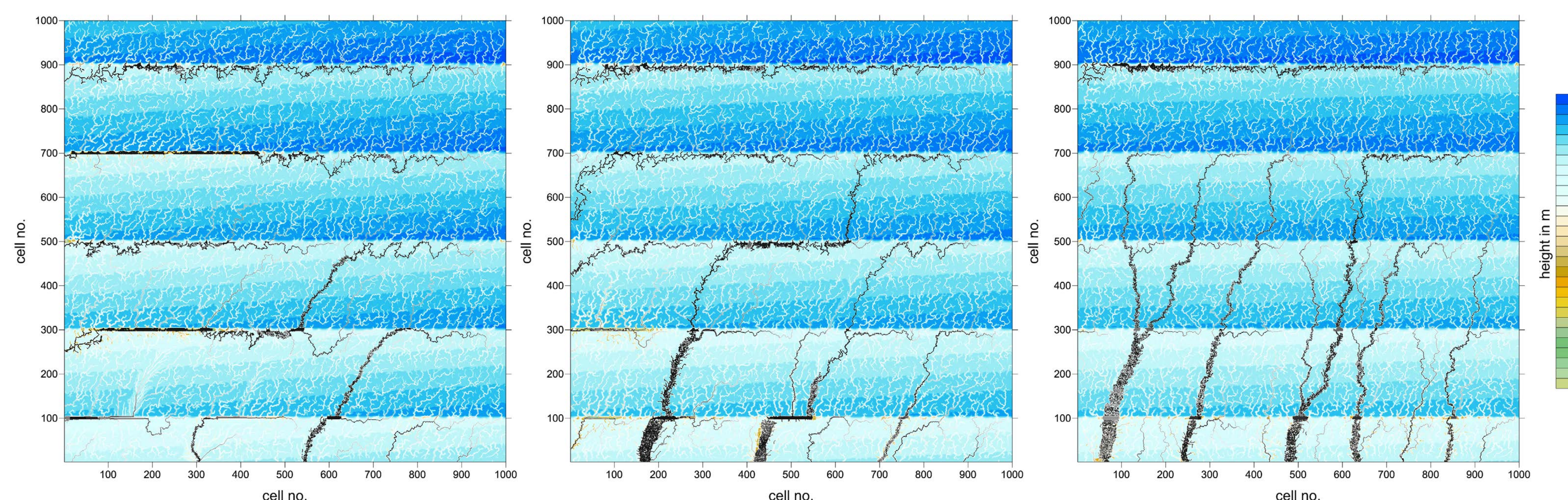


Fig.7: Simulated topographies of a developing river network after 25.000y of uplift and surface evolution. The main rivers are marked in black. The angle between rivers and faults varies from 60° on the left, to 70° in the middle and finally to 80° on the right. The incision rate and all other parameters are adopted from fig.6, middle.

### References

- O'Callaghan and Mark (1984), Computer Vision, Graphics and Image Processing 28, 323-344
- Roering et al. (1999) Water Resources Research 35, 853- 870
- Tachikawa et al. (2011) IEEE, 3657-3660
- Beaumont et al. (2001) Nature 414, 738-742
- Popov and Sobolev (2008), PEPI 171, 55-75
- Pysklywec (2006) Geology 34, 225-228.
- Planchon and Darboux (2001) Catena 46, 159-176
- Willett (2009) Tectonophysics 484, 168-180
- Beaumont et al. (1992) Thrust Tectonics, 1-18
- Willett (1999) IGR 104, 28957-981